Quart. J. R. Met. Soc. (1976), **102**, pp. 395–404

551·515.81(87)

Structure and motion of tropical squall-lines over Venezuela

By A. K. BETTS, R. W. GROVER and M. W. MONCRIEFF

Department of Atmospheric Science, Colorado State University, Fort Collins, Colorado

Atmospheric Physics Group, Physics Department, Imperial College, London

(Received 24 June 1975; revised 12 November 1975)

SUMMARY

The characteristics of squall-lines observed during the second Venezuelan International Meteorological and Hydrological Experiment (VIMHEX–1972) are compared with the predictions of Moncrieff and Miller (1976). These squall-lines are highly organized, propagate in a distinctive fashion, and effect a significant modification on both the thermodynamic and dynamic structure of the synoptic-scale flow. The predicted propagation speeds and transport properties are similar to those observed, although some significant differences are also apparent.

1. INTRODUCTION

The importance of convective systems in maintaining the thermodynamic structure of the tropical atmosphere has long been recognized (e.g. Riehl and Malkus 1958). Moreover, the larger scale fields appear to have an important control on convective transports. It has also been recognized that deep convection can be forced by the larger scale fields, for example, by low level convergence (Ooyama 1964; Charney and Eliassen 1964) which destabilizes the atmosphere. The role of wind shear in organizing severe storms in mid-latitudes was discussed by Ludlam (1963). Thus, the interaction between the large-scale fields, which can force and control deep convection in a number of ways, and the convective transports and sources of heat, water and momentum which in turn modify the large-scale fields, is a very complex one. Recent convective parameterization theories (Betts 1973a; Arakawa and Schubert 1974) have suggested that through this interaction, a balanced state exists in which there is a quasi-equilibrium between the convection and the large-scale fields on the time-scale of the large-scale processes. The formal concept that the convective atmosphere exhibits a characteristic structure has in fact been recognized for some time (Ludlam 1966).

Betts (1974) has qualitatively extended the formalism for modelling this scale interaction by distinguishing two ways in which the large-scale fields may control convection. The first is a control by the structure of the large-scale environment, which appears to determine what type of convection occurs; a static control since it is determined by the large-scale structure at a given time. For example, the stratification and the shear field can influence the depth of the convective layer and also the structure of the vertical transports and source terms. However, the static fields do not directly determine the magnitude of the convective transports nor, say, the number of clouds of a given type. If some quasi-equilibrium condition exists, the magnitude of the transports is determined by a second control through the dynamic or time-dependent large-scale fields which are forcing the convection. This was called a time-dependent control. (The term 'dynamic control' could also be used but it might be taken to exclude large-scale forcing processes such as the radiative fields.) The time-scale involved here is that of the large-scale changes.

This paper is concerned with the static type of control. Moncrieff and Green (1972) considered this aspect in their discussion of the propagation and transfer properties of a

type of steady, two-dimensional convection which they found could occur for a limited range of values of a large-scale nondimensional number (R). This type of convection was found to have features in common with mid-latitude squall-lines. A second class of analytic solutions can be identified (Moncrieff and Miller 1976) which describe a steady, propagating convective system, occurring at larger values of R, and which appeared to have most of the dynamical characteristics and transfer properties of tropical squall-lines. The purpose of this paper is to attempt a comparison of this theory for a propagating squall-line with observations of tropical squall-lines over land. We shall examine the environmental structure associated with these squall-lines, and the transformation of the atmosphere which they produce, as well as compare their propagation speeds with those predicted by the theory. The comparison is not straightforward for several reasons.

The dynamical model discussed in Moncrieff and Miller (1976) (hereafter abbreviated MM) involves the organized overturning and transformation of the atmosphere throughout the entire depth occupied by the convective system as this propagates through a region. It predicts the propagation speed for this system in terms of the convective available potential energy of the inflow for certain idealized atmospheric structures, in which there is inflow into the system at all levels in front and outflow to the rear. It also predicts the dynamic and thermodynamic modification of the atmosphere behind the squall-line in terms of inflow structure. However, the model assumptions and the structure of the Venezuelan squall-lines differ in several respects. First, the dynamical model assumes constant shear while the prevailing flow over Venezuela has a maximum easterly wind at about 650 mb with westerly shear above to high levels, but easterly shear below (see Fig. 5 and section 3). Second, the theory deals with the case of inflow in the front and outflow to the rear at all levels; the observations do show inflow in the front at all levels and outflow to the rear at low and high levels but also show weak inflow from 800 to 900 mb in the rear. The observed downdraught circulation is a low level feature with the main outflow in the lowest 100 mb, unlike the deep downdraught from the high troposphere, assumed in the dynamical model. The observed inflow and outflow structure more closely resembles the numerical simulation in MM rather than the idealized dynamic model.

The third problem of comparison between observations and theory relates to the coupling of meso- and synoptic-scale processes. Although developing perhaps in a region of convergence in the synoptic-scale flow, the dynamics and precipitation processes of the squall-line produce a small zone of strong convergence and divergence, which controls the local changes of the atmosphere. This interaction is poorly understood, and this Venezuelan data from a single station is inadequate to present a complete meso-synoptic analysis. We shall simply present the local transformation of the atmosphere shown by single station observations and compare these qualitatively with the analysis of MM.

Despite these several differences, the observed squall-lines do propagate at speeds close to those predicted by the simple theory and they do transform the whole atmosphere in a way which is qualitatively similar to that predicted by the theoretical model and the numerical integration. The limitations of this present steady model make fully quantitative comparisons with the real atmosphere unrealistic but even so the comparisons are remarkable and seem to justify further theoretical development and atmospheric comparisons.

2. Observations

(a) *Experiment*

From June to early September, 1972, the second Venezuelan International Meteorological and Hydrological Experiment (VIMHEX-1972) was conducted in northern Venezuela

during the rainy season. At the main experiment site at Carrizal (9°22·8′N 66°55·0′W) were located a GMD-1 rawinsonde system capable of frequent soundings, a 10 cm calibrated weather radar (an extensively modified M-33 radar with a 2° beam-width paraboloidal antenna), and a surface meteorological station. Forty rain-gauges were located within a circle of radius 60 km from the radar site. The radar was used to track storms that developed within 90 km of Carrizal, and to observe their life-cycle and top heights. Precalibrated radiosondes (Betts 1973b) were launched every 75–90 minutes to measure the structure of the atmosphere before, during and after the passage of storm systems. A number of major squall-line systems were observed during the summer. In four cases, a good line sample through them was obtained which was representative of the inflow into the squall-line.

Unfortunately there were not enough other rawinsonde observations in the area to adequately define a synoptic field over Venezuela.

(*b*) *Data processing*

A radar camera-scope recorded the echo positions at a series of attenuations and step elevations of the antenna (up to echo top or 60°) every fifteen minutes. From the microfilm, the echo life history was reconstructed. A mean storm track was determined from the sequence of echo positions, as were echo areas and top heights. The radar statistics for the summer are presented in Betts and Stevens (1974).

Each rawinsonde sounding was interpolated to 25 mb after computing standard meteorological variables (temperature, mixing ratio, hydrostatic height, potential temperature, equivalent potential temperature, saturation equivalent potential temperature, wind speed and direction). For the comparison with the theory, winds relative to each storm were computed and resolved in coordinate axes along the transverse to the storm motion vector.

(*c*) *Squall-line selection*

Grover (1974) examined all storm systems which had line-type characteristics, and identified a class which appeared to be true squall-lines. This class had similar geometric line structure, a distinct squall front, and effected a large thermodynamic and momentum modification on the synoptic flow. Moreover, apart from storm 47, the cumulonimbus cells within the lines moved in the same direction as the lines themselves, at least as far as discernible from the radar data. Table 1 presents some mean characteristics for these

TABLE 1. CHARACTERISTICS OF SOME TROPICAL SQUALL-LINES

Storm number	Major axis (km)	Minor axis (km)	Maximum area (km²)	Maximum height	Lifetime (min)	Observed path length (km)	Travel	
							Speed $m s^{-1}$	Direction (deg)
16	88	20	1290	13·3	165	150	16·4	094
27	96	32	2390	12·0	200	136	15·0	079
*35	90	46	3290	15·6	240	131	10·7	085
*47	120	27	2550	9·9	211	170	15·3	065
*60	95	20	1470	9·5	215	161	13·8	095
*64	100	30	2350	14·8	140	154	15·5	079
mean	98	29	2223	12·5	195	150	14·2 (Vector Mean)	083

The storm direction is in the usual meteorological notation for winds, i.e. 090° is a storm motion from east to west. The asterisk denotes the storms used in compositing the atmospheric transformation by the squall-line. The major and minor axes roughly indicate the storm envelope.

squall-lines. The variation in top heights is interesting. Storms 27, 35 and 64 had radar top heights very close to the thermodynamic equilibrium height for parcels rising from the subcloud layer (Grover 1974). However, storms 47 and 60 had much lower radar tops than parcel equilibrium heights. In the case of storm 60, a likely explanation was the extremely high shear in the upper troposphere (35 m s^{-1} from 300 to 150 mb), but no reason is apparent for the low top height of storm 47. It is possible that a potentially serious error in the radar measured cloud tops exists with a 2° beam width due to the detection by the side lobes at higher elevations of higher reflectivity regions lower down (Atlas 1964). This error is proportional to radar range, reaching 1½ km at a 60 km range. No independent means is available to determine the actual size of this error except that the general agreement between radar and adiabatic cloud tops suggests that it is not serious.

3. Comparison of theory and observations

The steady-state model developed in MM shows that the propagation speed, c, of a squall-line relative to the mid-level wind, U_M, is a function of the convective available potential energy, $CAPE$, but only weakly influenced by the inflow wind field ($c = C - U_M$ where C is the speed relative to the earth). For the constant shear case considered in MM, this weak dependence on the windfield appears in the non-critical effect of R, on the propagation speed and momentum modification (Figs. 2 and 3 of MM). The effect of the variation of mean density with height, appearing as the ratio of the convective scale-height, H, to the density scale-height, H_0, through the parameter $D = H/H_0$, is also small. For constant shear, the propagation speed relative to the earth is

$$C = U_M + \alpha\sqrt{CAPE} \qquad (1)$$

where α is a function of R and D, given in Fig. 2(b) of MM. For ranges of D and R typical of cumulonimbus convection the variation of α is only some 20%, within the observational error margin.

The undisturbed wind profile in the VIMHEX squall-line data typically has a reversal of wind shear at about the 3 km level, with easterly shear below and westerly shear above. However, although this is not a situation which can be represented by constant shear, in view of the weak R dependence, the values of α corresponding to the constant shear case are expected to be useful; although, clearly, solutions for profiles closer to those observed would be desirable. The value of α corresponding to $D = 1$ and $R = 4$ was chosen as representative of the storm data set, giving a prediction formula of

$$C = U_M + 0{\cdot}32\sqrt{CAPE} \qquad (2)$$

The available potential energy was calculated as follows. The observed cloud-top heights were in general agreement with pseudo-saturated ascent from the sub-cloud layer and evidently the squall-line transports this air to the upper troposphere without significant mixing. The available potential energy was calculated as the energy released by pseudo-saturated ascent at the mean equivalent potential temperature (θ_e) of the sub-cloud layer, neglecting the unrepresentative surface value. In effect, this value of θ_e was the average over the 980–900 mb layer. Hence for practical purposes the definition of convective available potential energy is

$$CAPE = \int_{z_b}^{H} g(\Delta\theta/\theta)\, dz \qquad (3)$$

where $\Delta\theta$ is the potential temperature difference at height z between the above pseudo-saturated adiabat and the environment at the same level; θ the ambient potential tempera-

ture at that level; z_b and H are cloud base and the equilibrium level of the adiabatic parcel respectively. This energy is proportional to the positive area on a thermodynamic diagram, assuming the above saturation adiabat.

(a) *Propagation speed*

The values of $CAPE$ and U_M appropriate to each of the squall-line cases were calculated from the VIMHEX data and the predicted propagation obtained from Eq. (2). The observational test of the analytic prediction formula, Eq. (2), is shown on Fig. 1 and Table 2. The error in the predicted speed, due to the error in calculating $CAPE$ from observations, and the error in the observed speed, were both estimated at $\pm 1\frac{1}{2}$ m s^{-1}. It is possible that errors in the observed propagation speed may be considerably greater than this because the value used assumes that the system propagated continuously with the same dynamical structure throughout the period of observation. However, it is clear from the numerical simulations of MM that during the growth period, the structure and propagation can be significantly different from the mature stage. It is not possible to estimate this additional source of error with any reliable accuracy.

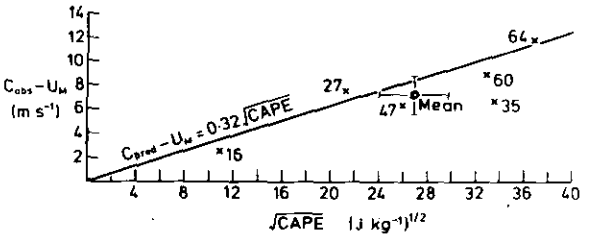

Figure 1. Observational test of the prediction formula $C_{obs} - U_M = 0{\cdot}32\sqrt{CAPE}$. The straight line represents the theoretical result.

In view of the differences between the observational wind fields and the constant shear of the theory, this cannot be taken as a definitive test of theory; rather, Fig. 1 suggests that further comparisons and development of the theory may be fruitful.

TABLE 2. COMPARISON OF THEORY AND OBSERVATION

Storm number	Available potential energy ($CAPE$) J kg^{-1}	Observed speed (C_{obs})	Predicted speed (C_{pred})	Midlevel windspeed (U_M)	$\sqrt{CAPE}$	$C_{obs} - U_M$	C_{obs}/C_{pred}
16	123	16·4	17·5	14·0	11·1	2·4	0·94
27	453	15·0	14·8	8·0	21·3	7·0	1·01
*35	1118	10·7	14·7	4·0	33·4	6·7	0·73
*47	676	15·3	17·3	9·0	26·0	6·3	0·88
*60	1080	13·8	15·5	5·0	32·9	8·8	0·89
*64	1363	15·5	15·8	4·0	36·9	11·5	0·98
Mean	802	14·5	15·9	7·3	26·9	7·1	0·91

All speeds are in m s^{-1} and related to the earth.
NOTE: The values of $CAPE$, and hence the predicted propagation speeds for storms 47 and 60, are an overestimate, since these were calculated using the adiabatic cloud top heights, which were much higher than the radar tops (section 2(c)).

(b) *Transformation of the atmosphere*

An important feature of the steady-state model is the marked transformation effected

on both the thermodynamic and dynamic state of the synoptic-scale fields. With a wind field of the form characteristic of the VIMHEX data, where low-level easterlies change over to upper-level westerlies with a maximum easterly flow around about the 3 km level, the model demands that easterly momentum is increased in low levels and westerly momentum increased in high levels, particularly in the anvil outflow. This model feature is shown in Table 1 of MM.

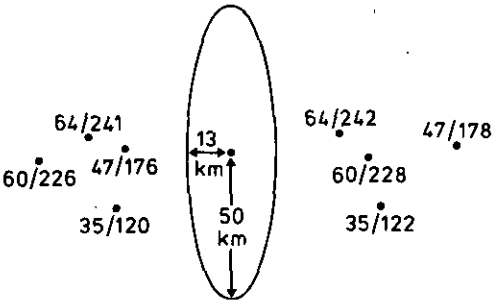

Figure 2. Relative positions of the radiosondes measuring the atmospheric structure before the squall-line (the inflow structure) and after its passage (mostly outflow – see Fig. 5) for the cases used in the composite. The respective storm and radiosonde numbers are marked.

The transformation of the atmosphere evident from the squall-line data was determined using the four cases for which a good line cross-section was obtained. Fig. 2 schematically shows the position of the radiosonde soundings relative to the squall-line systems. It was hoped that these four pairs of soundings in front of and behind the squall-line would be sufficiently representative of the unmodified inflow and unmodified outflow. They were averaged to give mean profiles of potential temperature, θ, equivalent potential temperature, θ_e, mixing ratio r, and velocity components along and transverse to the propagation direction, u_n, u_t respectively. It was considered to be more representative to average the soundings rather than generalize a particular case into a model because averaging minimizes variability in the data without smoothing these common features of the data set used as bases for selection.

Figs. 3 and 4 show the thermodynamic change and Fig. 5 the relative flow along and

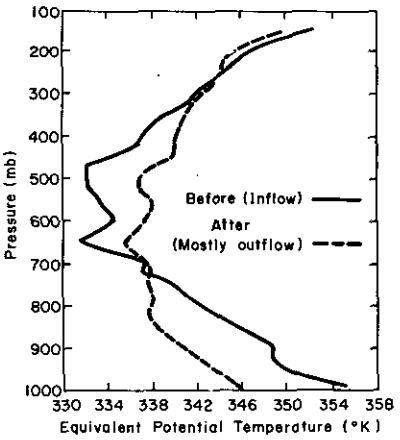

Figure 3. Modification of the equivalent potential temperature of the synoptic-scale flow composited from storms 35, 47, 60 and 64. The average time of the 'before' average was 1620 h (local time), and of the 'after' average 1833 h.

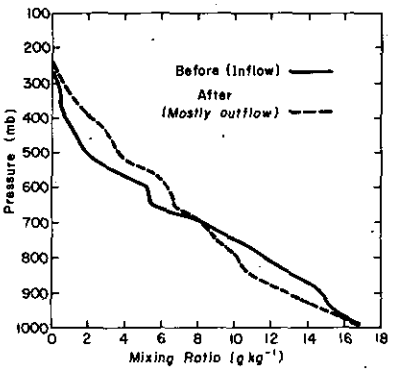

Figure 4. As Fig. 3, for mixing ratio.

transverse to the squall-line motion. Fig. 5 shows that the average flow in front of the squall-line is inflow at all levels in agreement with the theory. However, the relative flow, u_n, after the squall-line passage is not all outflow, as required by the analytic model. The mean relative flow, u_n, is near zero from 650 to 750 mb and small ($\simeq 2\,m\,s^{-1}$), but towards the squall-line, from 800 to 900 mb. The surface layer and the layer from 200 to 600 mb show outflow. There are also changes in the relative transverse flow indicating that the three-dimensional structure is important. The origin of the air in the apparent weak inflow from 800 to 900 mb is unclear and cannot be determined from this two dimensional analysis. This weak inflow may even result from an inappropriate estimate of the squall-line travel speed. These speeds were determined over as large a section of the lifecycle as was observed because accurate values over short time periods could not be estimated from the radar. The numerical simulations of MM show that the system propagation speed and the origin of the downdraught air changes as the system develops and attains a quasi-steady state. In these simulations there is partial inflow at the rear during the growing and dissipating stages, but total outflow during the quasi-steady, mature stage. Unfortunately, it is not

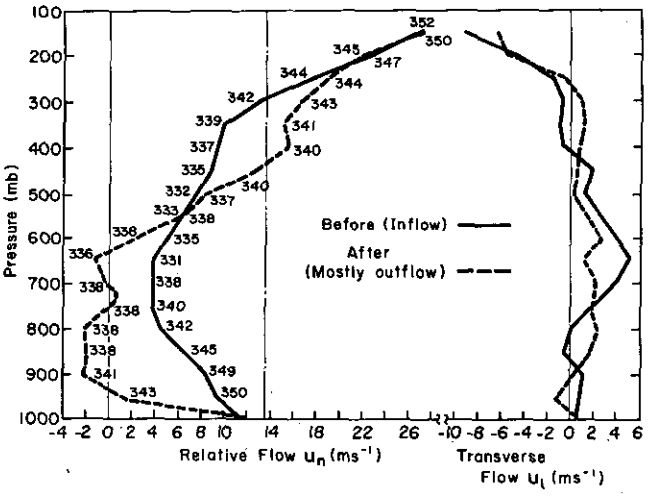

Figure 5. As Fig. 3 for along and transverse flow relative to the average squall-line motion vector (080° at 13·6 m s^{-1}): that is, the plus u_n axis (corresponding to a relative wind nearly from the west) has an earth orientation of 080°, and plus u_t of 350°. The dash-dotted vertical line represents the average propagation speed. Corresponding values of θ_e are printed alongside the normal relative flow curves.

possible to establish whether Fig. 5 represents an average behaviour over different regimes of the squall-line lifetime, in which case the error in the propagation speed is effectively greater, or whether partial inflow at the rear existed throughout the system lifetime.

Another problem is that some ambiguity exists between the speed of individual cells and that of the squall-line system. The attempt was made to determine the system velocity, which in some cases appeared to be lower than that of individual cells. These aspects need further study, perhaps with other data sets.

The transformation of the atmosphere by the passage of the squall-line cannot, therefore, be regarded as a simple inflow–outflow picture. Fig. 6 presents a schematic of the implied two-dimensional flow. Nonetheless, with inflow in the front at all levels, it seems appropriate to regard the squall-line as responsible for the transformation of the atmosphere.

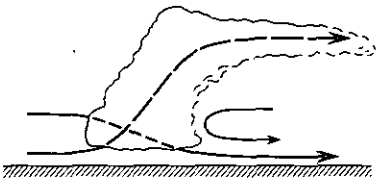

Figure 6. Schema of the relative airflow, u_n, normal to the major axis of the composite squall-lines, deduced from the composite data.

The modification of the θ_e profile in Fig. 3 shows that potentially-warm boundary layer air has been transported into high levels and replaced by potentially-cold air from mid-levels – effectively an overturning of the troposphere. Except in the lowest 150 mb, where a large cooling occurs (7 degC at the surface, falling to zero by 825 mb) and at high levels, this θ_e change is dominated by a mixing ratio change (Fig. 4).

The mixing-ratio profiles in Fig. 4 show that the downdraught transport of air of lower θ_e has resulted in a decrease in mixing ratio over the bottom 300 mb. The air above 700 mb has been moistened, a further indication that this air originated from the boundary layer. These changes in mixing ratio, although of considerable magnitude, in fact almost balance. Since there was appreciable rainfall, this balance indicates that the convergence of moisture into the system almost equalled the rainfall.

The change in the synoptic-scale windfield is very marked (Fig. 5), with a significant increase of easterly momentum in lower levels. Moreover, westerly momentum has been increased in upper levels. The obvious mass imbalance suggests again that three-dimensional effects are significant. In particular, the divergence in the low-level outflow is probably underestimated by the two-dimensional relative flow, u_n.

4. Limitations of this Study

It is worth noting that there are some important aspects of the observations which the analytic model cannot adequately describe. One of these is the unrealistic treatment of the downdraught, since in the analytic model, for reasons of mathematical tractability, it is assumed that the downdraught originates from high levels, whereas in the real squall-lines it is more likely to come from the lower atmosphere (as in the numerical simulation presented in MM). On the other hand, the updraught circulation is treated quite realistically. Another significant difference arises from the model achieving mass balance on the cloud scale, whereas the observations suggest that a significant element must be compensated for on the synoptic scale. Moreover, in some of the model solutions, the updraught and

downdraught are practically symmetric around the mid-level. This implies that since there is no moisture convergence, the potential energy for the downdraught circulation must balance the energy release in the updraught, and hence, an unrealistic total evaporation of precipitation. A simple estimate from the raingauge network gave an average precipitation in the squall-line rainfall carpet of 10 mm.

It could also be argued that since the observed squall-lines are associated with a synoptic-scale convergence, perhaps the atmospheric changes across the squall-line partly reflect synoptic-scale gradients concentrated by the mesoscale system. One study by Krishnamurti and Kanamitsu (1973) of a Caribbean easterly-wave shows a strong moisture gradient across the wave with dry subsiding air before the wave axis and moist ascending air with (parameterized) deep convection behind the wave axis. However, this moisture pattern was only noticeable during the VIMHEX-1972 experiment with the strongest disturbance of the summer which was preceded by a marked drying. The squall-lines presented here followed a day of diurnal convection and were preceded by a moist, high θ_e, sounding. Further, the north–south wind change (transverse component in Fig. 5) associated with the squall-line passage, does not appear to be consistent with the passage of a low-level trough in the easterlies. In the absence of adequate synoptic data, the relationship of meso- and synoptic-scale structure cannot be resolved.

Despite the significant differences between the analytic theory and the observations in the vertical mass transports, the predicted propagation speeds and transport properties are similar to those observed. This suggests that the updraught dynamics is fundamental and well represented by the theory. This may be in contrast to other convective circulations such as small cumulus which are probably controlled basically by thermodynamic and sub-cloud-scale properties. To understand this more fully, a more detailed comparison between time-dependent, three-dimensional simulations and observational case studies, perhaps linked to a modified thermodynamic representation in the analytic model, is necessary. This aspect is, however, beyond the scope of this paper.

5. Conclusions

Considerable agreement is found between the steady-state analytic model predictions and observed characteristics despite significant differences in outflow profiles and overall vertical mass transport. The analytic treatment could be extended to consider more complicated cases, but it would be more useful perhaps to compare observed data with further numerical simulations of the form of those in MM. The role of the analytic model is likely to be more valuable for assessing dynamical features such as the mechanical and thermodynamic efficiency of the transfer and providing a theoretical basis for further simulation and observation studies.

A general conclusion is that the tropical squall-line represents a convective process of a highly organized type, dominated by dynamical constraints. Both data and theory show that this type of convection is an important process for transporting mass, heat and momentum. These transport processes need to be considered in budget and prognostic studies of the tropical atmosphere. The relationship between meso- and synoptic-scale fields remains, however, unresolved.

Acknowledgments

This research was supported by the Atmospheric Science Section of the National Science Foundation under Grant OCD 72–01406. The VIMHEX-1972 field experiment was additionally supported by the Office of Naval Research under Contract No. 014–68A–

0493–002, the Facilities Laboratory of the National Center for Atmospheric Research, and the Meteorological Service of the Venezuelan Air Force.

We wish to thank Richard Miller and Polly Martin for their assistance in data reduction and Martin Miller for his comments. Mitchell Moncrieff acknowledges the hospitality of the Department of Atmospheric Science, Colorado State University, and the financial support of the National Science Foundation and The Royal Society. We thank referees who clarified the text.

References

Arakawa, A. and Schubert, W. 1974 Interaction of cumulus ensemble with the large-scale environment, Pt. I, *J. Atmos. Sci.*, **31**, pp. 676–701.

Atlas, D. 1964 Advances in radar meteorology, *Advances in Geophysics*, pp. 317–478.

Betts, A. K. 1973a Non precipitating cumulus convection and its parameterization, *Quart. J. R. Met. Soc.*, **99**, pp. 178–196.

1973b Precalibration of the VIZ–NWS radiosonde, *Bull. Amer. Met. Soc.*, **54**, pp. 222–223.

1974 The scientific basis and objectives of the U.S. convection subprogram for the GATE, *Ibid.*, **55**, pp. 304–313.

Betts, A. K. and Stevens, M. A. 1974 Rainfall and radar echo statistics. Venezuelan International Meteorological and Hydrological Experiment, 1972, *Research Report*, Atmospheric Science Department, Colorado State University, Fort Collins, Colorado.

Charney, J. G. and Eliassen, A. 1964 On the growth of the hurricane depression, *J. Atmos. Sci.*, **21**, pp. 68–75.

Grover, R. W. 1974 Characteristics of tropical squall-lines on Venezuela, *Atmospheric Science Report No. 228*, Colorado State University, Colorado.

Krishnamurti, T. N. and Kanamitsu, M. 1973 A study of a coasting easterly wave, *Tellus*, **25**, pp. 568–585.

Ludlam, F. H. 1963 Severe local storms: a review, *Met. Mon., Amer. Met. Soc.*, **5**, pp. 1–30.

1966 Cumulus and cumulonimbus convection, *Tellus*, **18**, pp. 687–698.

Moncrieff, M. W. and Green, J. S. A. 1972 The propagation and transfer properties of steady convective overturning in shear, *Quart. J. R. Met. Soc.*, **98**, pp. 336–352.

Moncrieff, M. W. and Miller, M. J. MM 1976 The dynamics and simulation of tropical squall-lines, *Ibid.*, **102**, pp. 373–394.

Ooyama, A. 1964 A dynamical model for the study of tropical cyclone development. *Geofisica International Mexico*, 4, pp. 187–198.

Riehl, H. and Malkus, J. S. 1958 On the heat balance in the equatorial trough zone, *Geophysica*, **6**, pp. 505–538.